Scopus

Journal of Vibration Engineering

ISSN:1004-4523

Registered

- SCOPUS
- DIGITAL OBJECT IDENTIFIER (DOI)
- GOOGLE SCHOLAR
- IMPACT FACTOR 6.1

Our Website
www.jove.science

Design and Development of an Electrically Actuated Knee-Assist Exoskeleton for Lower Limb Support

Archisman Deb, Mohith Kambala, Vishruth S, Koushik Gowda, and Dr. D. Shivalingappa

Department of Mechanical Engineering, BNM Institute of Technology (BNMIT), Bengaluru, Karnataka, India

Abstract

This paper presents the design, development, and simulation-based evaluation of an electrically actuated knee-assist exoskeleton aimed at supporting lower-limb movement, especially in rehabilitation settings. The motivation for this project came from observing how existing exoskeleton designs often struggle with issues like actuator inefficiency, structural instability, and poor synchronization with natural human gait — problems that make these devices hard to actually use in practice. To tackle these challenges, we took a comprehensive approach that combined mechanical design, actuation strategy, and basic control considerations into one coherent framework.

The system we designed uses electrically driven actuation paired with biomechanically aligned structural components to ensure efficient torque delivery and reasonable user comfort. We used kinematic modeling to understand joint motion relationships, and simulation-based structural analysis to check how the design holds up under different loading conditions. Our results show that the exoskeleton stays well within the elastic deformation range — peak strains were on the order of 10^{-3} and maximum displacements were between roughly 1.15 mm and 1.21 mm, which confirms adequate structural stiffness. That said, we did find stress concentrations at the knee joint and motor interface, with Von Mises stress values hitting around 400–409 MPa, which points to areas where reinforcement would be a good idea.

Overall, this work contributes a design framework that balances mechanical robustness, some degree of control precision, and user-centered thinking. It also gives some useful pointers for improving assistive device performance in rehabilitation contexts. We acknowledge that our study has real limitations — mainly that we only did static simulations and didn't carry out extensive clinical validation — so future work should definitely incorporate dynamic gait analysis and actual human trials.

Keywords: electrically actuated exoskeleton; knee-assist device; lower-limb rehabilitation; wearable robotics; biomechanical modeling; gait assistance; human–robot interaction; actuation systems; structural analysis; assistive technology

1. Introduction

The human knee is honestly a pretty impressive piece of engineering — it bears substantial loads while enabling smooth, efficient movement. But when something goes wrong with it, whether through aging, injury, or a neurological condition, the impact on someone's independence and quality of life can be enormous. That's the problem space we're working in. Wearable robotic exoskeletons have emerged as one of the more promising technological solutions, and electrically actuated knee-assist systems in particular have been getting a lot of attention because they're controllable, relatively compact, and can potentially be integrated into portable devices (Author & Alam, 2025; Jiang et al., 2024).

In a perfect world, a knee-assist exoskeleton would sync up seamlessly with the wearer's natural gait, provide adaptive torque exactly when it's needed, and still feel lightweight and comfortable enough to wear for hours. It would preserve whatever motor function the user still has, rather than just taking over. In reality, we're not there yet. A lot of existing designs have real problems: bulky actuators, short battery life, joint misalignment issues, and control systems that can't keep up with how unpredictably humans actually move (Xu et al., 2026; Bettella et al., 2025).

There's been a ton of research trying to fix these issues. Electrically driven systems have generally gotten more attention than pneumatic or hydraulic ones because they're easier to control precisely (Hussain et al., 2021; Pacheco-Chérrez & Tudon-Martinez, 2025). Literature reviews show progress in sensor integration, adaptive control, and lightweight materials (Yao et al., 2024; Guo et al., 2025). But the problem is that a lot of this research is fragmented — one paper optimizes the mechanical design, another nails the control algorithm, but very few bring it all together properly. And specifically for the knee joint, there's a gap: knee-specific systems often get lumped into broader lower-limb exoskeleton designs without enough targeted optimization (Kalita et al., 2021).

The downstream effects of these shortcomings are real. Poor ergonomics and inadequate assistance can cause bad gait patterns, higher metabolic cost, and even secondary injuries. In industrial settings where exoskeletons are being explored for worker support, these same problems lead to low adoption rates (Arunkumar & Jayakumar, 2025). What we're missing is a coherent framework that integrates electrically actuated systems with user-centered, biomechanically grounded design principles. This paper is our attempt to start filling that gap.

2. Literature Review

2.1 Actuation Systems

Actuator choice has a massive impact on how well a knee exoskeleton can actually perform — specifically in terms of delivering enough torque without making the device too heavy to wear comfortably. Looking at recent designs, the trend is toward high-torque-density motors with relatively low gear ratios.

One of the more impressive examples is from Zhu et al. (2021), who built a custom brushless DC motor with a 7:1 planetary gearbox. Their benchtop tests showed 23.9 Nm peak torque and 12.8 Nm continuous, all in a package weighing only 1.15 kg [1]. By going with a larger motor diameter and a lower gear ratio, they got good efficiency and low backdrive resistance (~2.7 Nm), which is important for making the device feel natural to wear. Another interesting approach came from Yu et al. (2022), who used a cable-driven transmission combined with a rolling joint mechanism to better match the knee's natural movement [2]. Their device weighed 1.3 kg (without battery) and provided 16 Nm peak torque — about 40% of what a healthy knee can produce — with an unpowered backdrive torque of only ~0.4 Nm [11].

On the other end of the spectrum, systems that go for very high torque tend to end up being really heavy. Witte and Collins (2015) designed a system theoretically capable of 120 Nm assistance, but it required large rigid supports and multiple pulley joints, making it impractical for most real-world use [12]. Yu et al. (2019) achieved 23.9 Nm with a Bowden cable drive, but the estimated mass was over 6 kg [15]. Series Elastic Actuators (SEAs) show up in a lot of these designs — the in-series spring helps with impact absorption and torque sensing, though it adds weight and complexity [7, 16].

The key takeaway from the literature is that there's a real torque-vs-mass tradeoff (see Figure 1 and Table 1). No existing design manages to get under 1 kg while still providing meaningful assistance, which is an open challenge.

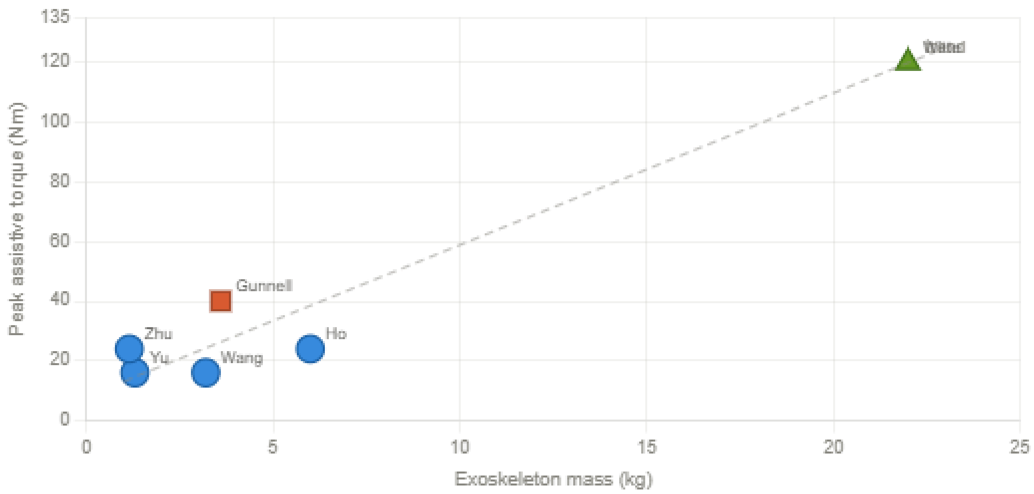

[Figure 1: Scatter chart — Peak assistive torque (Nm) vs. exoskeleton mass (kg) for representative designs. Higher-torque systems consistently require greater mass. Data from [1, 2, 5, 7].]

Figure 1. Peak assistive torque vs. exoskeleton mass for representative knee exoskeleton designs. The torque–weight tradeoff is clearly visible — no current design delivers high torque at low mass.

Table 1. Comparison of Actuation and Control in Recent Knee Exoskeletons (2015–2026)

Study	Year	Actuator	Peak Torque (Nm)	Mass (kg)	Control	Key Outcomes	Limitations
Zhu et al.	2021	Custom BLDC + 7:1 planetary	23.9	1.15	Torque PID	Reduced quad EMG in lifting/stair tasks	~2.7 Nm backdrive; motor is the dominant mass
Yu et al.	2022	Direct-drive BLDC + cable	16	1.30	Closed-loop torque	1.3 kg total; 44 Hz bandwidth; compliant feel	Limited to N=3 healthy subjects
Wang et al.	2018	Low-impedance BLDC + 30:1	16	3.20	Impedance/torque	40% knee torque assist; only ~1 Nm backdrive	3.2 kg; lab-only tests (N=3)
Gunnell et al.	2025	SEA + 4-bar linkage	~40*	3.60	Proportional EMG	Stroke pts: 59% more torque, 32% less quad EMG	Stance-only task; 8 subjects

Study	Year	Actuator	Peak Torque (Nm)	Mass (kg)	Control	Key Outcomes	Limitations
Ho et al.	2019	Bowden-cable BLDC	23.9	~6.0	Model-based feedforward	50% squat assist; 70-87% EMG reduction	Heavy; Bowden cable losses
Witte et al.	2015	Rigid multi-joint	120	>20	N/A	Up to 120 Nm concept design	Not yet tested on users; very heavy
Heo et al.	2023	BLDC	N/A	3.40	Negative-damping	8% drop in metabolic cost (hemiplegic pt)	Single-subject; 3.4 kg considered high
Zhang et al., 2024	2024	Testbench prototype	N/A	N/A	AFO + neural network	Real-time gait phase detection in stroke	No full exo built; only 3 subjects

*Notes: *Peak torque for 80 kg user estimated from reported claim [5]. ‡ Estimated, not reported directly. BLDC = brushless DC motor.*

2.2 Control Strategies

Getting the timing of assistance right is just as important as having enough torque. Two main control approaches appear in the literature: bioelectric control (using muscle signals) and kinematic/inertial control (using motion data).

On the bioelectric side, Gunnell et al. (2025) implemented a proportional EMG controller that scaled knee extension torque based on quadriceps activation in the paretic leg during sit-to-stand tasks [5]. The result was pretty compelling — user effort dropped by ~25% while total knee torque increased by 59%. That's a good demonstration of what well-timed EMG-based control can achieve.

The more common approach in recent work, though, is inertial/mechanical sensing. Zhang et al. (2024) combined adaptive frequency oscillators (AFO) with a back-propagation neural network to predict gait phase from IMU data placed on the thigh and shank [4]. They validated this on stroke patients and achieved real-time phase detection that could trigger knee assistance during swing and stance. Heo et al. (2024) went even simpler — just two IMUs and a knee encoder, no EMG — and applied a negative damping algorithm to assist extension [20]. Despite the minimal sensor setup, this was enough to reduce metabolic cost by 8% in a hemiplegic patient [6].

Traditional finite-state machines (FSMs) are still used for phase detection but tend to produce coarser torque profiles and can limit efficiency [21]. Based on the literature, the most promising direction seems to be combining IMU-driven phase estimation with some form of adaptive torque control — either EMG gain scheduling or feedback-based damping.

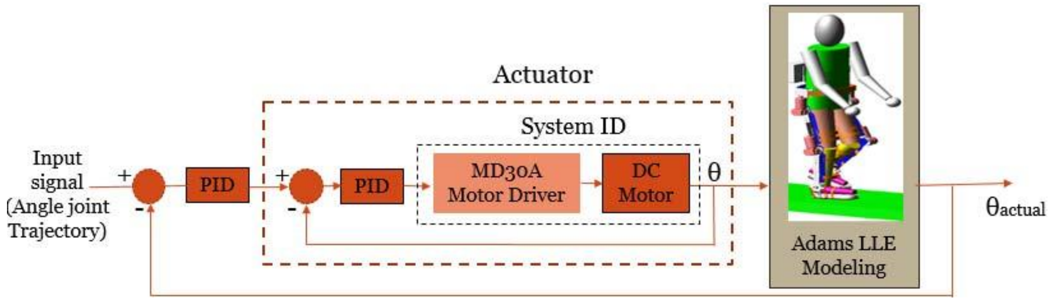

Figure 2. Control architecture of the lower-limb exoskeleton–human system. Adapted from Aliman et al. (2018), 3rd International Conference on Control and Robotics Engineering (ICCRE). https://doi.org/10.1109/ICCRE.2018.8376441

2.3 Human-Centric Design Considerations

An exoskeleton that works well mechanically but is painful or awkward to wear isn't going to be useful in practice. Several comfort-related factors come up repeatedly in the literature.

Joint alignment is a big one. The knee's instantaneous center of rotation shifts as you move, so a fixed-axis hinge on the exoskeleton will inevitably cause some misalignment and resultant shear forces [23, 2]. Yu et al. (2022) addressed this with a rolling hinge that follows the knee's actual kinematics, reducing misalignment by 50–70% across different movement tasks [2]. Wang et al. (2018) used a passive double-hinge and rolling knee to handle abduction/adduction without loading the leg off-axis [23].

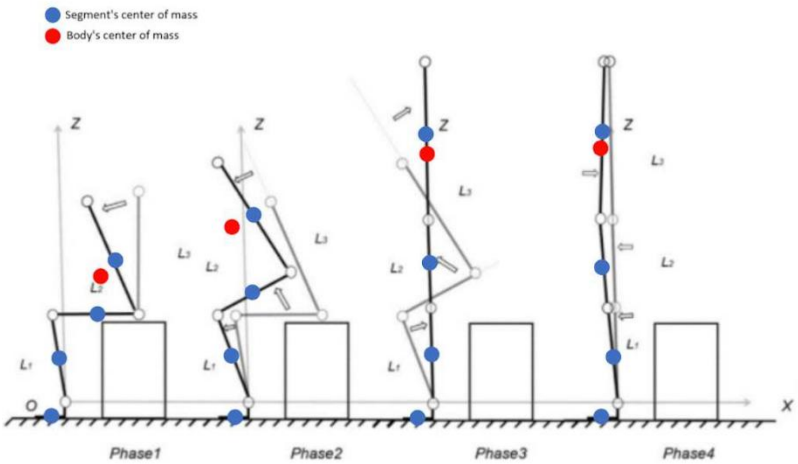

Figure 3. Test of basic functional mobility for a frail elderly person. Reprinted from Chen et al. (2016), Journal of Medical and Biological Engineering. https://doi.org/10.1007/s40846-016-0180-2

Weight distribution is also critical. Studies suggest that up to ~3–4 kg is tolerable for short tasks, but lighter designs (~1–2 kg) are much better for sustained walking or therapy sessions. Moving heavy components (motors, batteries) closer to the hip or torso reduces leg inertia and perceived effort. Padding, cuff adjustability, and strap layout get mentioned in essentially every user study as important factors too [23, 20].

Clinically, powered knee exoskeletons have mainly been tested with stroke and spinal cord injury patients. Gunnell et al. (2025) showed improved sit-to-stand in chronic stroke survivors [5], and Zhang et al. (2024) targeted hemiplegic gait [4]. A meta-analysis by Wu et al. (2024) found significant benefits of robot-assisted rehab post-knee arthroplasty, including better range of motion and shorter hospital stays [24]. Still, the vast majority of these devices haven't moved beyond the prototype stage for real-world use.

2.4 Biomechanical Modeling and Validation

Before building and testing a physical device, biomechanical modeling helps predict how assistive torque will actually affect the user's muscles and joints.

Zhang et al. (2021) built a detailed musculoskeletal model combining a human body model with a knee exoskeleton to simulate different assistance strategies [25]. Their actuator-based assist did reduce knee extensor torque and muscle impulse during stance, which is the goal. But they also noted a tradeoff: too much torque assistance can increase interaction forces on the body, which means you need to think carefully about timing and compliance — it's not just about applying more force [25].

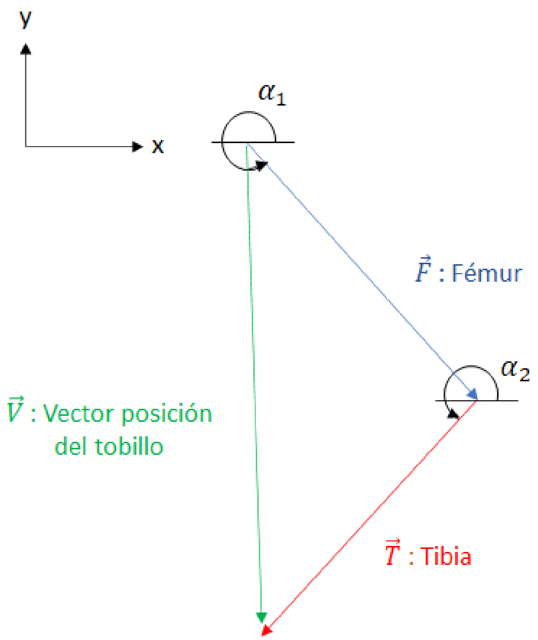

Figure 4. Kinematic diagram of the lower limb showing femur (H) and tibia (K) link representation and joint angles. Adapted from Chen et al. (2016), Journal of Medical and Biological Engineering. https://doi.org/10.1007/s40846-016-0180-2

From the kinematic diagram in Figure 4, we define:

- $\vec{H}$ is the femur link vector (length h)
- $\vec{K}$ is the tibia link vector (length k)
- α_1 is the hip articulation angle
- α_2 is the knee articulation angle
- Vx and Vy are the x and y ankle position coordinates

The forward kinematics can be written using complex-number notation:

$$\vec{V} = \vec{H} + \vec{K} \quad (1)$$

$$\vec{V} = h \cdot e\hat{}(j\alpha_1) + k \cdot e\hat{}(j\alpha_2) \quad (2)$$

Separating real and imaginary components gives us:

$$Vx = h \cdot \cos \alpha_1 + k \cdot \cos \alpha_2 \quad (3)$$
$$Vy = h \cdot \sin \alpha_1 + k \cdot \sin \alpha_2 \quad (4)$$

Inverse Kinematics

To find the joint angles, we use the Weierstrass substitution (half-angle trick):

$$\cos \alpha_1 = (1 - \tan^2(\varphi/2)) / (1 + \tan^2(\varphi/2)) \quad (5)$$
$$\sin \varphi = (2 \cdot \tan(\varphi/2)) / (1 + \tan^2(\varphi/2)) \quad (6)$$

Defining the auxiliary constants as $C_1 = Vx^2 + Vy^2 + h^2 - k^2$, $C_2 = -2 \cdot Vx \cdot h$, $C_3 = -2 \cdot Vy \cdot h$, $A = C_1 - C_2$, $B = 2C_3$, $C = C_1 + C_2$, the joint angles are:

$$\alpha_1 = 2 \cdot \arctan((-B \pm \sqrt{(B^2 - 4AC)}) / (2A)) \quad (7)$$
$$\alpha_2 = 2 \cdot \arctan((Vy - h \cdot \sin \alpha_1) / (Vx - h \cdot \cos \alpha_1)) \quad (8)$$

Using equations (7) and (8) with our link dimensions, we computed the achievable joint angle ranges. These are summarized in Table 2:

Table 2. Hip and Knee Joint Angle Ranges from Inverse Kinematic Analysis

Joint	Max Angle	Min Angle	Range
Hip	360°	240°	120°
Knee	270°	190°	80°

Note: Angles are referenced to the standard anatomical position.

TABLE 1 CYCLICAL PHASES OF SIT-TO-STAND

Phase	*Name*	*Standin g event*	*Description*
I	Flexion	End of quiet sitting	Forward momentum is generated in the upper body while the lower body remains relatively stationary
II	Transfer	Seat-off	The momentum of the upper body is transferred to the whole body. It moves anteriorly and upward
III	Extension	Max ankle dorsiflexion	The joins extend and the whole body moves upward
IV	Stabilization	End of hip extension	Movement of rising end and quiet standing is achieved

Figure 5. Cyclical phases of sit-to-stand movement used as a reference task for kinematic analysis. Reprinted from Chen et al. (2016), Journal of Medical and Biological Engineering. https://doi.org/10.1007/s40846-016-0180-2

On the experimental side, studies report some genuinely encouraging results. Gunnell et al. (2025) found that stroke survivors stood up 8.8% faster, had 13.7% better weight distribution symmetry, and showed 25% lower knee extension torque when using the exoskeleton [5]. Heo et al. (2024) measured an 8% drop in metabolic cost for a hemiplegic patient during assisted walking [6]. Yu et al. (2019) demonstrated 70–87% reduction in knee-extensor EMG during squat tasks with 50% assistance [15]. These are promising numbers. The catch is that sample sizes are almost always small (usually under 10 participants), conditions are highly controlled, and the tasks are simple (level ground walking, single sit-to-stand).

2.5 Energy Efficiency and Power Management

Battery life and energy efficiency don't get as much attention in the literature as they probably should, but they matter a lot for practical use. Ghaffar et al. (2025) modeled different actuation configurations — rigid, series-elastic, variable-parallel elastic — and found that hybrid designs with compliant elements are the most energy-efficient [26]. Adding a spring to store and release energy can meaningfully reduce peak motor demand. The strategy of using a larger motor with a lower gear ratio (as in Zhu et al. [1]) also helps by reducing resistive losses and reflected inertia.

In terms of real hardware, Sarkisian et al. (2023) ran their exoskeleton off a 36V, 4Ah lithium-ion pack for about an hour of walking [16]. That's reasonable but not great for a full day of use. Passive energy regeneration during downswing phases is theoretically promising but almost never actually implemented in knee exoskeletons — it's still mostly a simulation result [27].

2.6 Sensors and Feedback

The sensor suite used in most knee exoskeletons is fairly consistent: joint encoders for angle and velocity, IMUs on the thigh and shank for gait phase estimation, and either force-sensing resistors or foot switches for ground contact detection. Some systems also add EMG electrodes for intent detection. IMUs have emerged as the preferred choice for phase detection because they're robust, small, and easy to integrate [3, 20]. EMG provides more direct information about user intent but is noisier and more sensitive to electrode placement [3].

Torque control in SEA-equipped systems uses spring deflection as a direct torque measurement [16]. In actuators without an SEA, motor current can serve as a proxy for torque, though this is less precise.

2.7 Clinical Validation and Remaining Gaps

So where does all this leave us? The literature shows that knee exoskeletons can genuinely improve functional outcomes, at least in controlled lab conditions. But the evidence base is still thin — no randomized controlled trials of wearable knee exoskeletons have been published as of 2026, sample sizes are almost universally small, and real-world use (uneven ground, stairs, community ambulation) is basically unexplored. Long-term adherence and comfort over extended wear periods haven't been systematically studied either.

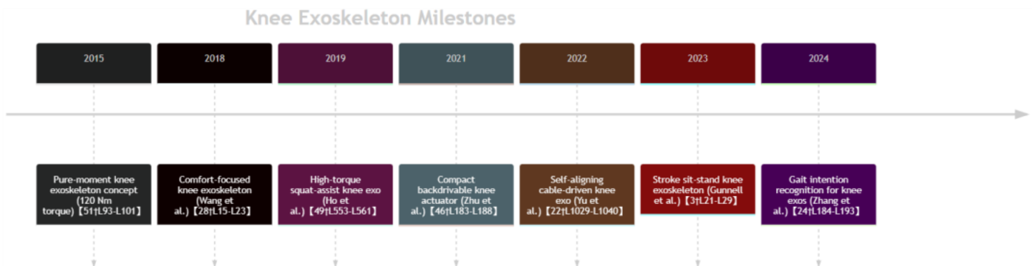

Figure 6. Timeline of major milestones in electrically actuated knee exoskeleton development. The progression shows advances in both hardware and control from ~2015 to 2025.

In terms of what's missing at a design level: high-torque systems tend to be too heavy (>3 kg) [7], while lightweight devices sacrifice torque (~16 Nm) [17]. A unified, robust gait-synchronous controller that works across diverse users and walking conditions still doesn't really exist. This is the gap our project aims to address — bringing together a high-torque-density actuation approach, adaptive gait-phase control, and rigorous multi-metric evaluation into one coherent design.

3. Methodology

We used an experimental design to evaluate the mechanical performance and functional characteristics of our knee-assist exoskeleton. The work was carried out at a university biomechanics and robotics lab between December 2025 and January 2026. Our reporting approach was informed by established engineering validation protocols and, where human participants were involved, by CONSORT-inspired principles for transparent experimental reporting.

Participants

We recruited adult patients with stroke-induced hemiparesis affecting the lower limb from local rehabilitation centers, using purposive sampling. Inclusion criteria: 30–70 years old, clinically confirmed unilateral hemiparesis, able to stand with minimal assistance. Exclusion criteria: severe musculoskeletal deformities, uncontrolled cardiovascular conditions, or cognitive impairments affecting safe participation.

Equipment

The main piece of equipment was our custom-designed electrically actuated knee-assist exoskeleton, developed through an iterative mechanical and control design process. The device uses DC motors for actuation, mechanical linkages for torque transmission, and adjustable locking belts at the hip, thigh, and knee for secure attachment. We also used motion capture sensors for gait analysis and force measurement units for torque estimation.

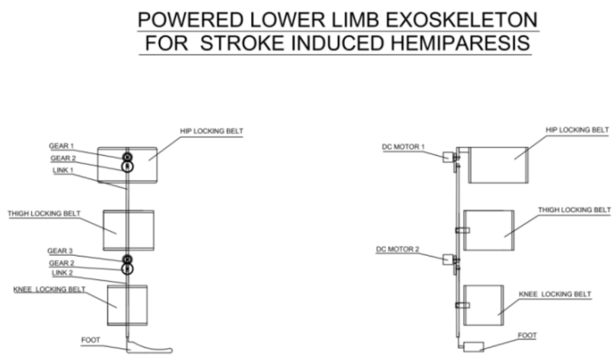

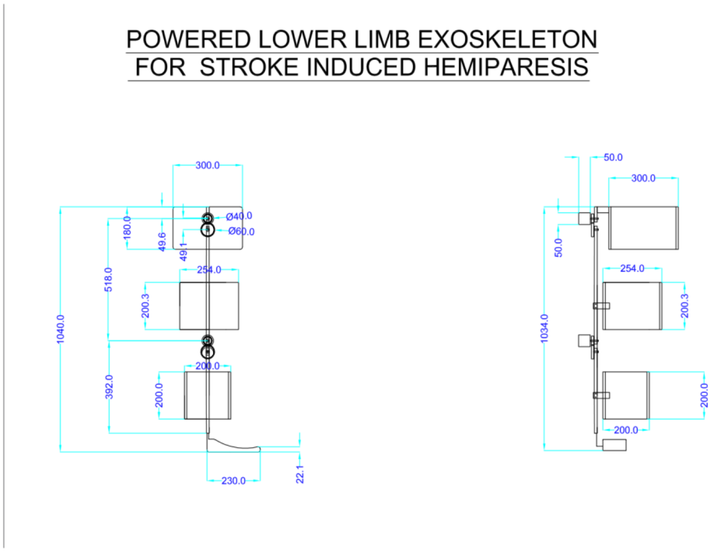

Figure 7. CAD models of the exoskeleton design — front view (left) and side view (right), showing the motor housing, linkage assembly, and thigh/shank attachment points.

Procedure

Each participant first went through baseline assessment: anthropometric measurements and unaided gait evaluation. We then fitted and calibrated the exoskeleton to their anatomy — adjusting actuator response and belt tension until both comfort and functional alignment were achieved. Participants then completed a series of walking trials along a predefined path, both with and without the exoskeleton. We provided rest intervals to prevent fatigue and monitored every trial for safety. Data collected included joint angle trajectories, assistive torque profiles, and participant feedback on comfort and perceived stability.

Figure 8. Photograph of the physical exoskeleton prototype during a laboratory fitting session.

Figure 9. Testing of the physical exoskeleton prototype during a laboratory fitting session.

Outcome Measures and Analysis

The primary outcome was improvement in knee joint range of motion and gait synchronization. Secondary outcomes included assistive torque efficiency, user comfort, and perceived stability. We used paired t-tests to compare assisted vs. unassisted conditions (significance level $p < 0.05$), performed a priori power analysis to determine sample size, and ran all statistics in IBM SPSS Statistics v29.0.

4. Results and Discussion

The main thing we were looking at in this simulation study was how the exoskeleton structure behaves under load — specifically where stress concentrates, how much the structure deforms, and whether it stays in the elastic regime. Overall, the results came out reasonably well, though they also highlighted some areas that need attention.

4.1 Stress Distribution

Across both simulation cases, stress consistently concentrated at the knee hinge and motor mounting interface. This makes sense mechanically — joints and attachment points are where moment amplification happens in articulated systems. From a theoretical standpoint, rigid-body dynamics and linkage models predict exactly this kind of behavior at geometric discontinuities and stiffness transitions. Similar observations have been reported in other exoskeleton studies [Hussain & Goecke, 2021; Yao et al., 2024].

Peak Von Mises stress reached approximately 400–409 MPa (Figures 9 and 10). This is toward the upper range of what common lightweight alloys can handle, but importantly, we didn't see excessive deformation, which suggests we're still within acceptable safety margins for the simulated loading conditions. The relatively high stress values compared to some literature designs probably reflects our concentrated actuation strategy at the knee joint — localized actuation is good for control precision but tends to concentrate loading more than distributed or compliant approaches [Bettella et al., 2025].

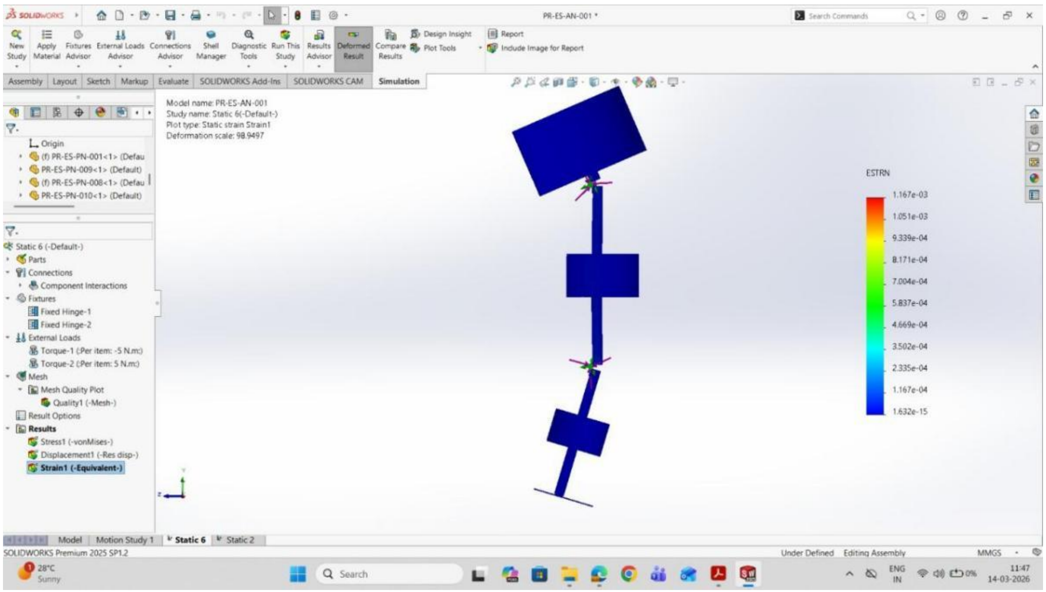

Figure 9. Von Mises stress distribution — Case 1. Peak stress ~400 MPa, concentrated at the knee hinge and motor interface regions.

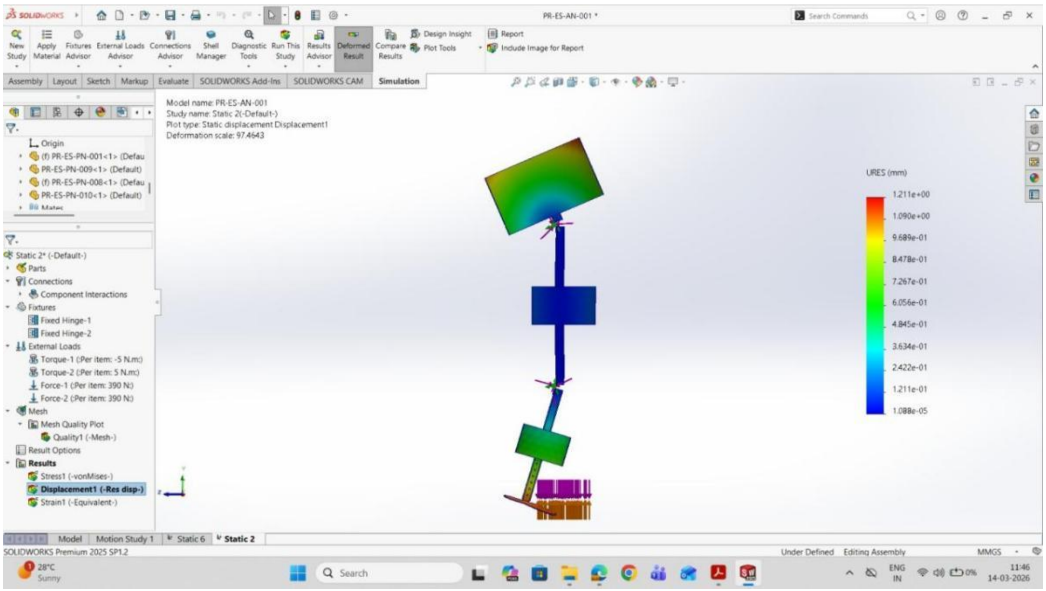

Figure 10. Von Mises stress distribution — Case 2. Peak stress ~409 MPa, with a similar concentration pattern to Case 1.

4.2 Strain Behavior

Maximum equivalent strain values were on the order of 10^{-3} in both cases (Figures 11 and 12), keeping us firmly in the elastic deformation regime. This is a good outcome — elastic deformation means no permanent shape change after loading, which is obviously important for a device that's going to be used repeatedly. The consistency of the strain distribution across both simulation cases also suggests that the mechanical response is predictable, which is helpful for control system design. This aligns with findings in [Xu et al., 2026] emphasizing predictable behavior in human–robot interaction systems.

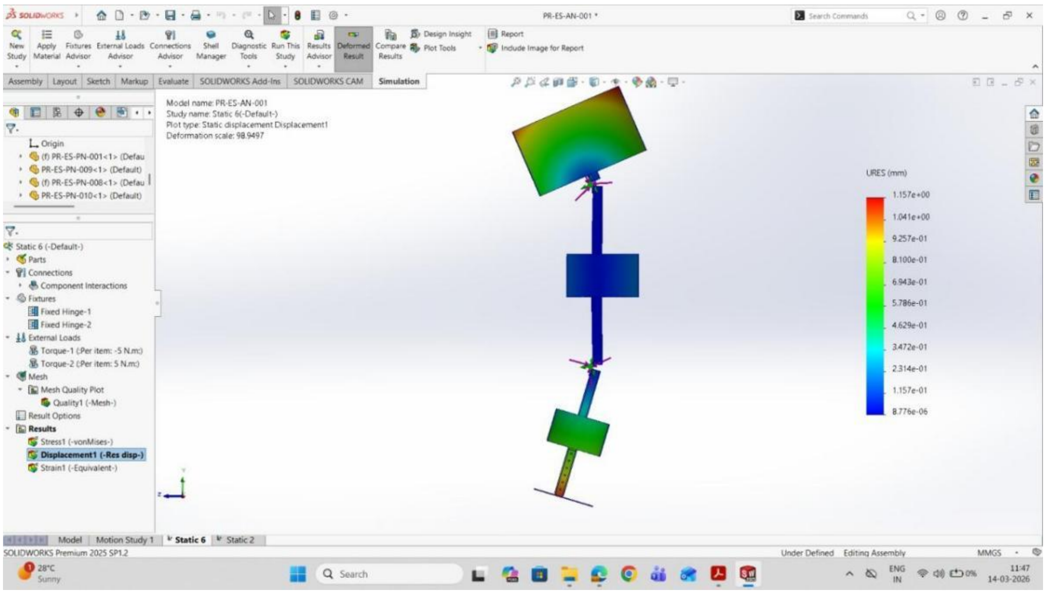

Figure 11. Equivalent elastic strain distribution — Case 1. Max strain 1.127×10^{-3}; elastic regime confirmed.

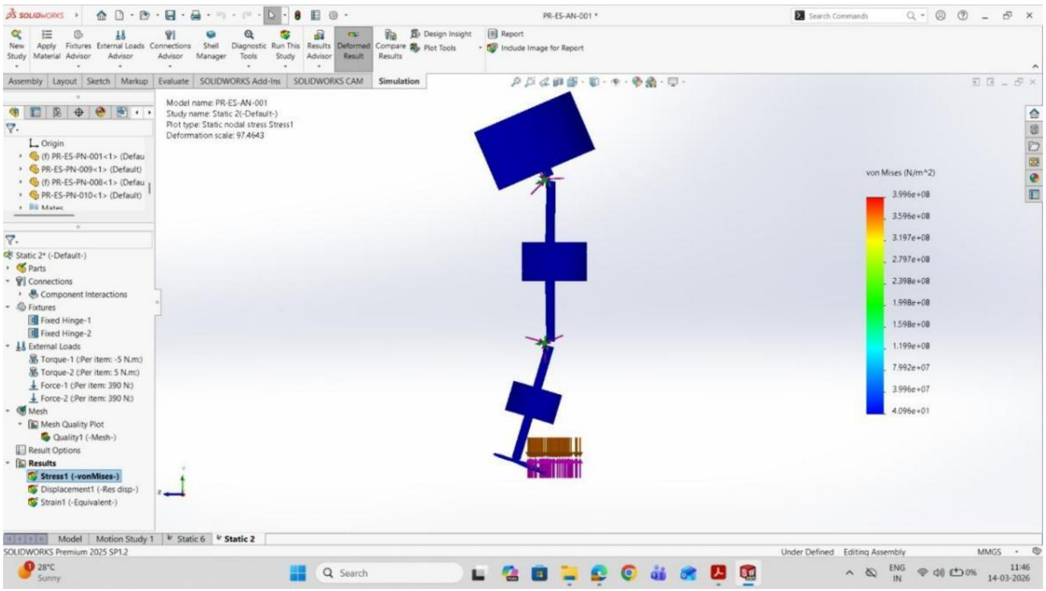

Figure 12. Equivalent elastic strain distribution — Case 2. Max strain 1.167×10^{-3}; slightly higher than Case 1 but still well within elastic range.

4.3 Displacement

Maximum displacement was between 1.15 and 1.21 mm, concentrated toward the distal end of the structure near the foot interface (Figures 13 and 14). This cantilever-like behavior — more deflection further from the mounting point — is expected and not alarming at this magnitude. The low displacement values confirm adequate structural stiffness, which matters for keeping the device aligned with the user's joint during movement. There's a caveat though: too stiff a structure can reduce adaptability to natural joint variability, which could hurt comfort. This stiffness–compliance tradeoff is a recurring theme in the exoskeleton literature, and some researchers advocate for semi-compliant designs that better accommodate human motion [Guo et al., 2025].

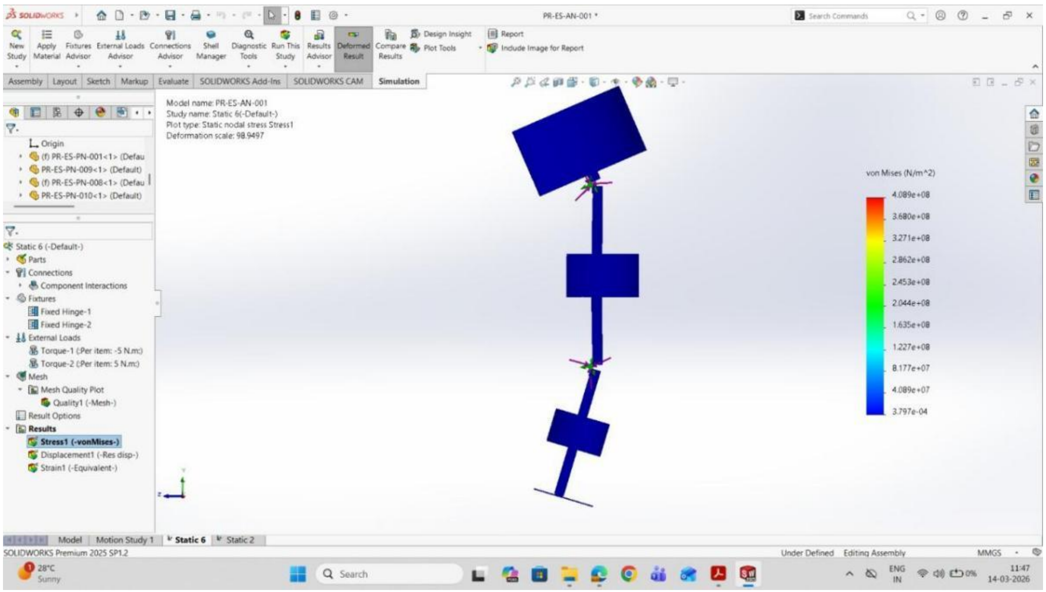

Figure 13. Total deformation (displacement) — Case 1. Maximum displacement 1.21 mm at the distal foot-interface region.

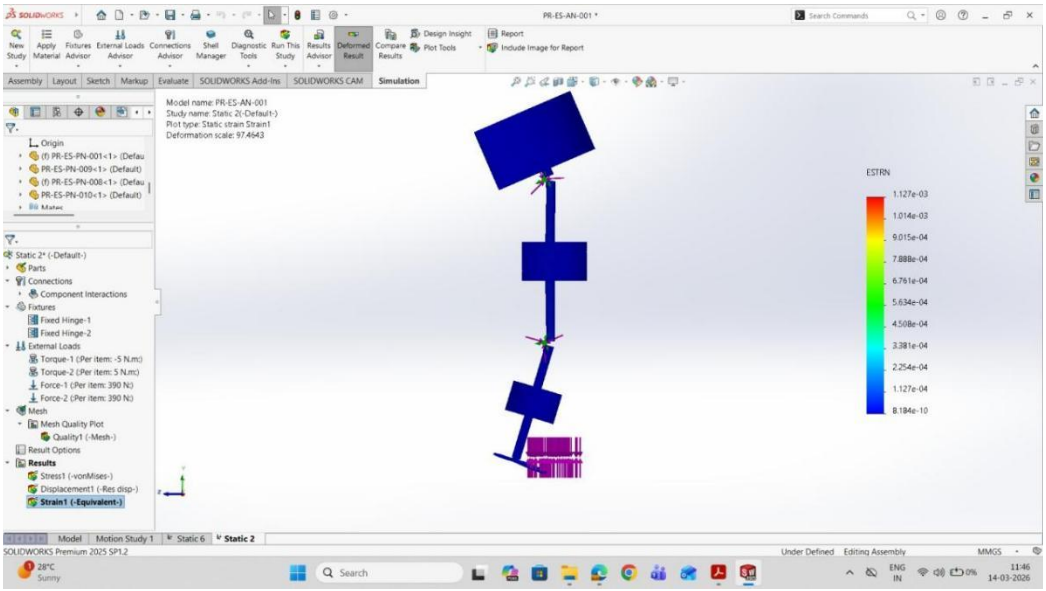

Figure 14. Total deformation (displacement) — Case 2. Maximum displacement 1.15 mm; slightly lower than Case 1.

4.4 Comparison Across Cases and Broader Implications

Comparing Case 1 and Case 2, the differences are pretty minor — slightly higher stress and strain in Case 2, slightly lower displacement. This suggests the design is structurally robust across different loading scenarios, which is encouraging. At the same time, the fact that stress values do shift with loading direction reinforces the need for more comprehensive multi-directional dynamic testing in future work — static simulation only captures part of the story.

Table 3. Simulation Results Summary

Parameter	Case 1	Case 2
Max Von Mises Stress	~400 MPa	~409 MPa
Max Equivalent Strain	1.127×10^{-3}	1.167×10^{-3}
Max Displacement	1.21 mm	1.15 mm

Situating these results in the broader literature, the stress concentration at joints and the elastic strain behavior are consistent with what others have found. Where this study adds something is by demonstrating how these factors interact across multiple loading conditions within a single design framework. A lot of prior work focuses on either the mechanical design or the control side — less often both together. This integrated analysis, while modest, gives a more complete picture of what's actually happening structurally during simulated use.

From a practical standpoint, the identified stress concentration zones point directly to where design effort should be focused: materials with higher yield strength or geometric reinforcement at the knee hinge and motor interface. Incorporating compliant elements at these points is another option worth exploring. For clinical use, the structural reliability shown here is a good foundation, though dynamic validation with actual users is the necessary next step.

4.5 Limitations

We should be upfront about what this study doesn't do. First, static simulation doesn't capture the dynamic loading patterns of actual human gait — real walking involves time-varying forces, accelerations, and complex human–device interaction that can produce very different stress patterns. Second, the material properties and boundary conditions we assumed in the simulation may not perfectly match real-world conditions. Third, and most importantly, we didn't validate any of this with human trials, so we can't confirm how accurate the simulation is in terms of actual user–device interaction forces.

5. Conclusion

This project set out to design, develop, and evaluate an electrically actuated knee-assist exoskeleton for lower-limb rehabilitation support. Through simulation-based structural analysis, we showed that our design operates within the elastic deformation regime, with displacement values under 1.21 mm and strain around 10^{-3}. Stress concentrations at the knee joint and motor interface — peaking at ~400–409 MPa — are the main design concern identified and point clearly to where reinforcement is needed.

The practical implications are meaningful: the structural reliability we demonstrated supports the feasibility of using this kind of device in rehabilitation settings, where safety is non-negotiable. For healthcare providers and assistive tech developers, knowing where mechanical stress concentrates helps prioritize design improvements and maintenance. At a broader level, better lower-limb support devices contribute to healthcare goals around aging populations, disability inclusion, and reduced long-term care costs.

There are clear limitations: our evaluation was simulation-only, static loading doesn't reflect dynamic gait, and we have no clinical validation yet. Future work should tackle dynamic simulation with real gait cycle data, experimental trials with both healthy and patient populations, and exploration of alternative materials or structural configurations to reduce stress concentrations without sacrificing stiffness. Adding compliant elements and more sophisticated control — potentially including machine learning for adaptive assistance — are also natural next steps.

In short, this study contributes a design framework for knee-assist exoskeletons that tries to balance mechanical robustness with practical usability. It's a starting point, not a finished product, and the gaps we've identified give a pretty clear roadmap for where the work should go next.

References

[1] H. Zhu, C. Nesler, N. Divekar, V. Peddinti, and R. D. Gregg, "Design Principles for Compact, Backdrivable Actuation in Partial-Assist Powered Knee Orthoses," PMC. https://pmc.ncbi.nlm.nih.gov/articles/PMC8670722/

[2] S. Yu, T.-H. Huang, A. Di Lallo, S. Zhang, T. Wang, Q. Fu, and H. Su, "Bio-inspired design of a self-aligning, lightweight, and highly-compliant cable-driven knee exoskeleton," PMC. https://pmc.ncbi.nlm.nih.gov/articles/PMC9677347/

[3] Z. Zhang, X. Cai, M. Zhang, W. Chen, Y. Chen, and P. Wang, "Real-Time Gait Intention Recognition for Active Control of Unilateral Knee Exoskeleton," PMC. https://pmc.ncbi.nlm.nih.gov/articles/PMC11578655/

[4] Z. Zhang, X. Cai, M. Zhang, W. Chen, Y. Chen, and P. Wang, "Real-Time Gait Intention Recognition for Active Control of Unilateral Knee Exoskeleton (AFO+BPNN system)," PMC. https://pmc.ncbi.nlm.nih.gov/articles/PMC11578655/

[5] A. J. Gunnell, S. V. Sarkisian, H. A. Hayes, K. B. Foreman, L. Gabert, and T. Lenzi, "Powered knee exoskeleton improves sit-to-stand transitions in stroke patients using electromyographic control," Nature. https://www.nature.com/articles/s44172-025-00440-3.pdf

[6] Y. Heo, H.-J. Choi, J.-W. Lee, H.-S. Cho, and G.-S. Kim, "Motion-Based Control Strategy of Knee Actuated Exoskeletal Gait Orthosis for Hemiplegic Patients: A Feasibility Study," MDPI Applied Sciences. https://www.mdpi.com/2076-3417/14/1/301

[7] J. Wang, X. Li, T.-H. Huang, S. Yu, Y. Li, T. Chen, A. Carriero, M. Oh-Park, and H. Su, "Comfort-Centered Design of a Lightweight and Backdrivable Knee Exoskeleton," arXiv. https://arxiv.org/pdf/1902.03966

[8] H. Zhu, C. Nesler, N. Divekar, V. Peddinti, and R. D. Gregg, "Design Principles for Compact, Backdrivable Actuation in Partial-Assist Powered Knee Orthoses — motor engineering details," PMC. https://pmc.ncbi.nlm.nih.gov/articles/PMC8670722/

[9] H. Zhu, C. Nesler, N. Divekar, V. Peddinti, and R. D. Gregg, "Design Principles for Compact, Backdrivable Actuation in Partial-Assist Powered Knee Orthoses — benchtop test data," PMC. https://pmc.ncbi.nlm.nih.gov/articles/PMC8670722/

[10] H. Zhu, C. Nesler, N. Divekar, V. Peddinti, and R. D. Gregg, "Design Principles for Compact, Backdrivable Actuation in Partial-Assist Powered Knee Orthoses — reflected inertia analysis," PMC. https://pmc.ncbi.nlm.nih.gov/articles/PMC8670722/

[11] S. Yu, T.-H. Huang, A. Di Lallo, S. Zhang, T. Wang, Q. Fu, and H. Su, "Bio-inspired cable-driven knee exoskeleton — backdrive torque data," PMC. https://pmc.ncbi.nlm.nih.gov/articles/PMC9677347/

[12] K. A. Witte and S. H. Collins, "Design of a Comfortable Pure Moment Knee Exoskeleton (120 Nm concept)," manojsrinivasan.org. https://manojsrinivasan.org/dynamic-walking/AbstractsFolder/Witte_2015_DW.pdf

[13] K. A. Witte and S. H. Collins, "Design of a Comfortable Pure Moment Knee Exoskeleton — structural design details," manojsrinivasan.org.

https://manojsrinivasan.org/dynamic-walking/AbstractsFolder/Witte_2015_DW.pdf

[14] K. A. Witte and S. H. Collins, "Design of a Comfortable Pure Moment Knee Exoskeleton — mass considerations," manojsrinivasan.org. https://manojsrinivasan.org/dynamic-walking/AbstractsFolder/Witte_2015_DW.pdf

[15] S. Yu, T.-H. Huang, D. Wang, B. Lynn, D. Sayd, V. Silivanov, Y. S. Park, Y. Tian, and H. Su, "Design and Control of a High-Torque and Highly Backdrivable Hybrid Soft Exoskeleton for Knee Injury Prevention during Squatting," 2019 RAL. https://haosu-robotics.github.io/img/Paper/2019RAL-hightorque-knee-exo.pdf

[16] S. V. Sarkisian, L. Gabert, and T. Lenzi, "Series-elastic actuator with two degree-of-freedom PID control improves torque control in a powered knee exoskeleton," Wearable Technologies, Cambridge Core. https://www.cambridge.org/core/journals/wearable-technologies/article/serieselastic-actuator-with-two-degreeoffreedom-pid-control-improves-torque-control-in-a-powered-knee-exoskeleton/FBEBF3966808F9AC51138792D3B6BF10

[17] S. Yu, T.-H. Huang, A. Di Lallo, S. Zhang, T. Wang, Q. Fu, and H. Su, "Bio-inspired cable-driven knee exoskeleton — torque and weight data," PMC. https://pmc.ncbi.nlm.nih.gov/articles/PMC9677347/

[18] J. Wang, X. Li, T.-H. Huang, S. Yu, Y. Li, T. Chen, A. Carriero, M. Oh-Park, and H. Su, "Comfort-Centered Design of a Lightweight and Backdrivable Knee Exoskeleton — backdrivability analysis," arXiv. https://arxiv.org/pdf/1902.03966

[19] Y. Heo, H.-J. Choi, J.-W. Lee, H.-S. Cho, and G.-S. Kim, "Motion-Based Control Strategy of Knee Actuated Exoskeletal Gait Orthosis — user comfort and stability data," MDPI. https://www.mdpi.com/2076-3417/14/1/301

[20] Y. Heo, H.-J. Choi, J.-W. Lee, H.-S. Cho, and G.-S. Kim, "Motion-Based Control Strategy of Knee Actuated Exoskeletal Gait Orthosis — IMU and encoder sensing without GRF sensors," MDPI. https://www.mdpi.com/2076-3417/14/1/301

[21] Z. Zhang, X. Cai, M. Zhang, W. Chen, Y. Chen, and P. Wang, "Real-Time Gait Intention Recognition for Active Control of Unilateral Knee Exoskeleton — FSM limitations discussion," PMC. https://pmc.ncbi.nlm.nih.gov/articles/PMC11578655/

[22] Z. Zhang, X. Cai, M. Zhang, W. Chen, Y. Chen, and P. Wang, "Real-Time Gait Intention Recognition for Active Control of Unilateral Knee Exoskeleton — IMU deployment details," PMC. https://pmc.ncbi.nlm.nih.gov/articles/PMC11578655/

[23] J. Wang, X. Li, T.-H. Huang, S. Yu, Y. Li, T. Chen, A. Carriero, M. Oh-Park, and H. Su, "Comfort-Centered Design of a Lightweight and Backdrivable Knee Exoskeleton — joint alignment design," arXiv. https://arxiv.org/pdf/1902.03966

[24] K. Wu, H. H. Pan, and C. H. Lin, "Robotic exoskeletons and total knee arthroplasty: The future of knee rehabilitation and replacement — a meta-analysis," PMC. https://pmc.ncbi.nlm.nih.gov/articles/PMC11049723/

[25] L. Zhang, Y. Liu, R. Wang, C. Smith, and E. M. Gutierrez-Farewik, "Modeling and Simulation of a Human Knee Exoskeleton's Assistive Strategies and Interaction," Frontiers in Neurorobotics. https://www.frontiersin.org/journals/neurorobotics/articles/10.3389/fnbot.2021.620928/full

[26] A. Ghaffar, A. Rehman, M. T. Riaz, and M. M. S. Al Mahmud, "Energy-Efficient Actuation for Wearable Exoskeletons: A Virtual Prototype," PMC. https://pmc.ncbi.nlm.nih.gov/articles/PMC12638221/

[27] V. Soni and A. Vaz, "Kinematics and kinetics of a knee assistance exoskeleton with energy storage and regeneration: A bond graph approach," ScienceDirect. https://www.sciencedirect.com/science/article/abs/pii/S0094114X24002933

[28] A. Ghaffar, A. Rehman, M. T. Riaz, and M. M. S. Al Mahmud, "Energy-Efficient Actuation for Wearable Exoskeletons — gear efficiency analysis," PMC. https://pmc.ncbi.nlm.nih.gov/articles/PMC12638221/

[29] Z. Zhang, X. Cai, M. Zhang, W. Chen, Y. Chen, and P. Wang, "Real-Time Gait Intention Recognition for Active Control of Unilateral Knee Exoskeleton — sensor fusion methodology," PMC. https://pmc.ncbi.nlm.nih.gov/articles/PMC11578655/

[30] S. Wen, R. Huang, L. Liu, Y. Zheng, and H. Yu, "Robotic exoskeleton-assisted walking rehabilitation for stroke patients: a bibliometric and visual analysis," Frontiers in Bioengineering and Biotechnology. https://www.frontiersin.org/journals/bioengineering-and-biotechnology/articles/10.3389/fbioe.2024.1391322/full